

Static study of a double pass solar air heater support

Oumaima Eleuch *, Badis Bakri, Zied Msaed, Zied Driss

Laboratory of Electro-Mechanic Systems (LASEM), National School of Engineers of Sfax (ENIS), University of Sfax (US),

B.P. 1173, Road Soukra km 3.5, 3038 Sfax, TUNISIA

Abstract: This work presents the design of a double pass solar air heater fixed on the wall by a four legs design pivoting system. In the case of supplying a building with hot air, for heating purposes, or for industrial applications such as drying or preheating, this pivoting mechanism consists of two supports with two legs linked to the collector itself and the fixing is ensured by two clevises. To make a static simulation of the pivoting mechanism, we use the CAD software Solid Works. According to the obtained results, we can approve that our support can bear the load of the solar collector and resist to weather conditions.

Key words: Double pass solar air heater, four legs design pivoting system, static simulation, Solidworks.

1. Introduction

The concept of solar air heating has been in use from many years. Heat from the sun stored in iron was utilized to heat a home in 1877 [1]. First design of solar air heater comes into light in 1881 which was a wall hung wooden framed cabinet consisting of a blackened metallic sheet covered with a transparent glass. In the literature, ONG [2] developed a mathematical model and procedure for predicting thermal performance of single pass solar air collectors. Bhushan et al. [3] evaluated thermal and thermo hydraulic performance of the roughened solar air heater having protruded absorber plate using a mathematical model. An analytical approach was used by Ammari [4] to develop a mathematical model for predicting the thermal performance of a solar air heater with slats. An exact analytical solution for fully developed convective heat transfer in rectangular ducts under a constant heat flux was derived by Shahmardan et al. [5]. Lee et al. [6] investigated the influences of several critical parameters on the thermal performance and outlet temperature of solar

collector. These results showed that the optimal configurations of the solar collector was identified, which is provided with high transmissivity glass, rectangular-tubes absorber plate, tilt angle of 45°, black polished surface, and airflow length of 4 m. Bassiouny and Koura [7] considered some geometric parameters, such as collector inlet size and width, which are believed to have a significant effect on space ventilation. Dović and Andrassy [8] developed different numerical models in order to assess the influence of design and operating parameters such as bond conductance between absorber plate and tube, tube diameter, glass cover to absorber plate distance, optical properties of absorber and flow rate on thermal efficiency of collectors.

The purpose of this study is to investigate the static simulation of a two-pass solar air heater support that assures the fixation of the collector in the wall and allows it to be pivoting and adjustable at a precise angle and remains it stable at this position.

2. Solar air heater design

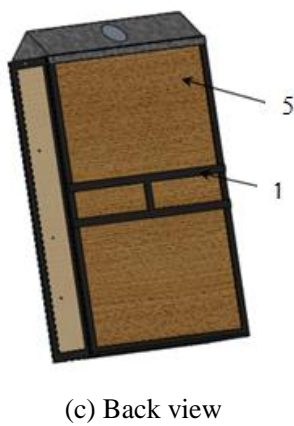
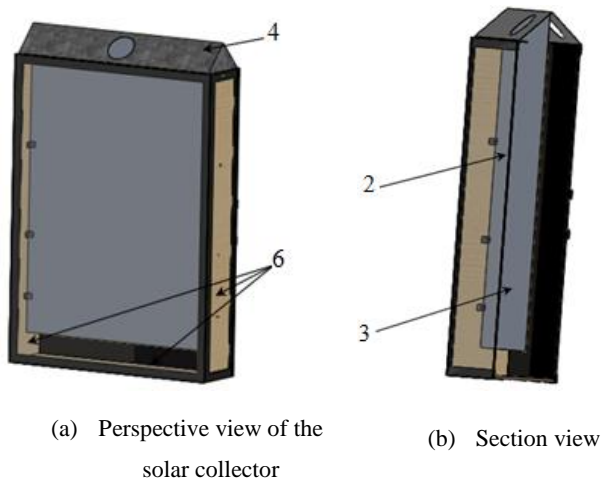
The solar collector consists essentially of a frame that determine the shape and the dimensions of the solar air heater and the absorber plate which has two

* **Corresponding author:** Oumaima Eleuch
E-mail: oumaimaeleuch@gmail.com.

major roles. Firstly, it absorbs most possible of the solar radiation and secondly it transmits the generated heat to the heat transfer fluid with a minimum of losses. The glazing consists of a transparent material. It is used to allow solar radiation to enter inside the solar air heater. In this solar collector, we have four sides to reduce the heat losses: left and right side, bottom side and back side. Finally, we have the inlet and the outlet where the air enters from one hole and pass through the heating chamber. Then, it will go out from the second hole. The solar air heater assembly is presented in figure 1.

N°	Designation	Material
1	Frame	Steel
2	Glazing	Glass
3	Absorber plate	Galvanized steel
4	Inlet and outlet unit	Galvanized Steel
5	Back insulation	Wood
6	Lateral insulation	Wood (MDF)

Fig. 1 Solar collector view



3. Installation configurations

The collector is attached to the wall and allows the supply of a building with warm air using ventilation system consisted on ducts and fan as shown in figure 2. The pivoting system of the solar air heater used in this configuration is the four legs design. This system is constituted by two supports with two legs linked in this case to the collector itself and the fixing is ensured by two clevises as shown in figure 3. These two clevises ensure both the pivoting and the positioning of the collector which makes it possible to have a tilt angle between 0° and 90° with a simple adjustment, easy and more precise, as illustrated in figure 4.

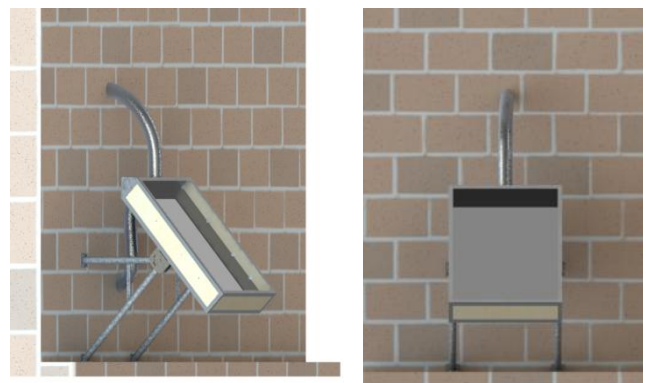
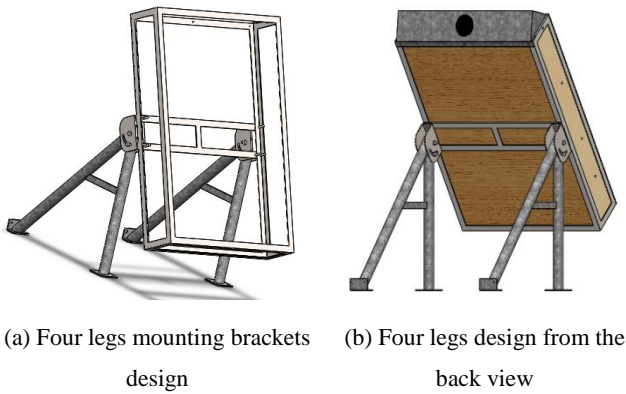
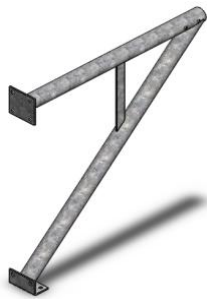


Fig. 2 Heating of a building

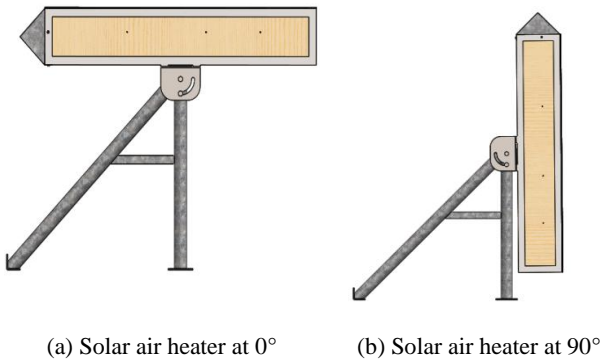


(a) Four legs mounting brackets design (b) Four legs design from the back view



(c) Two legs bracket

Fig. 3 Four legs design 3D views



(a) Solar air heater at 0° (b) Solar air heater at 90°

Fig. 4 Angle settings

4. Static study of the pivoting system

We are interested in this part on the static study of the four legs design pivoting system using Solidworks. In these conditions, the collector can pivot relatively to a support fixed on a wall.

4.1 Static analysis of the mounting brackets

The mounting brackets are solicited by several constraints. The collector with his weight which is near to 30 kg exerted a force of approximately 300 N.

For safety purpose, we need to consider the weather conditions effects such as wind effect. The force resulting from the action of the wind has two components, one called drag D which is parallel to the wind movement, and the other lift L which is perpendicular to the wind movement.

In this case, the drag force of the air is expressed as follow:

$$D = \frac{1}{2} C_x \rho V^2 S \quad (1)$$

where:

C_x : Drag coefficient equal to 1 in our case.

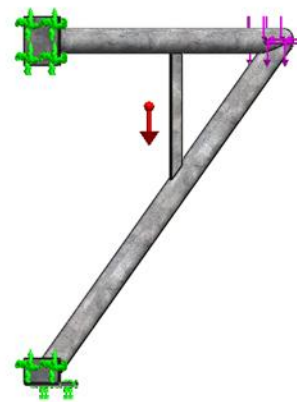
ρ : Air density equal to 1.29.

V : Air velocity equal to 100 km/h in case of violent wind.

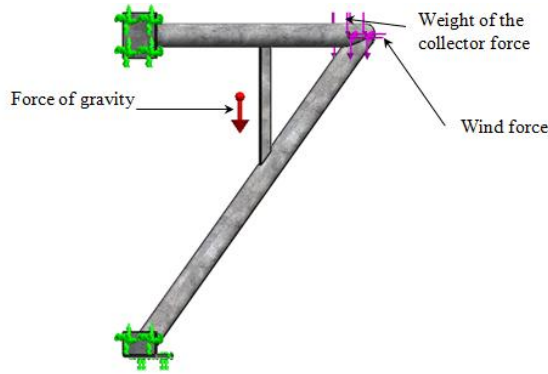
S : lateral surface of our collector equal to 0.22 m².

Consequently, the drag force of the air is equal to $D=105$ N.

A static simulation will take place to verify the resistance of our support in case of the solar collector fixed on a wall. Figure 5 shows clearly the boundary conditions consisting on the wind resultant force, the weight of the collector force and the gravity force. Figure 6 shows the meshing consisting of 22960 nodes and 11336 elements.



(a) Imposed displacements



(b) External loads

Fig. 5 Boundary conditions

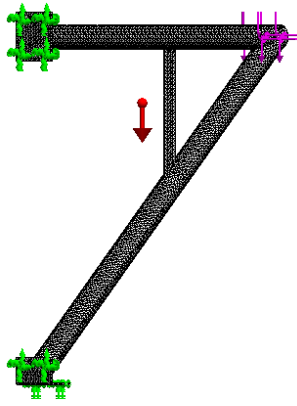


Fig. 6 Meshing

4.1.1 Displacement

Figure 7 shows the displacement distribution and indicates in red color the maximum displacement which is about 1 mm. This displacement is allowed regarding that this displacement occur only in case of severe weather conditions.

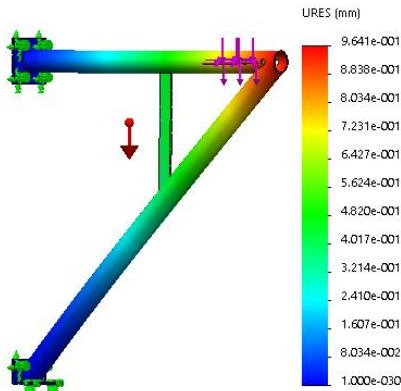


Fig. 7 Displacement distribution

4.1.2 Von Mises stress

Referring to the results provided by simulation in figure 8, we found that in areas of stress concentrations (having the red color), there is a maximum stress which is equal to $\sigma_{max} = 94 \text{ MPa}$. We can verify that:

$$\sigma_{max} < \sigma_{adm} = \frac{R_e}{s} \approx 100 \text{ MPa} \quad (2)$$

In these condition the safety coefficient is $s=2$. If we take into consideration that this system is studied in a very severe conditions (storm conditions), we can approve that our support can bear the load of the solar collector and resist to weather conditions.

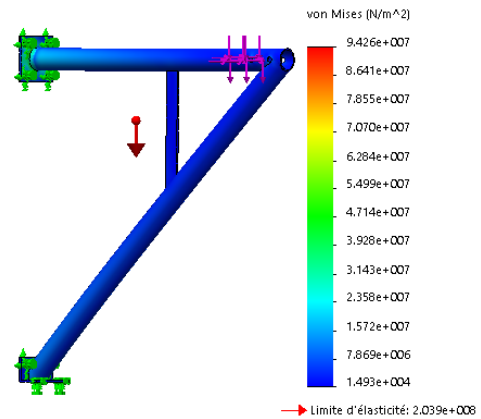


Fig. 8 Von Mises stress distribution

4.2 Static analysis of the clevis

In this section, we can ignore the wind effect because the lateral surface of the clevis is small and we are interested only in the load coming from the weight of the solar collector F which is equal to 300 N. Figure 9 shows the boundary conditions consisting of the imposed displacement and the external loads. Figure 10 shows the meshing consisting of 5997 nodes and 2862 elements.

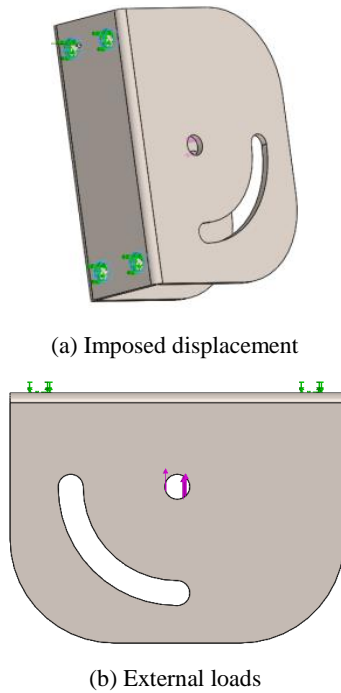


Fig. 9 Boundary conditions

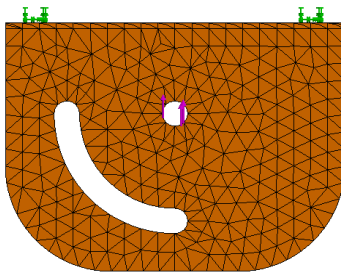


Fig. 10 Meshing

4.2.1 Displacement

Figure 11 shows the displacement distribution and indicates in red color the maximum displacement which is about 1 mm. This displacement is allowed regarding that this displacement occur only in case of severe weather conditions.

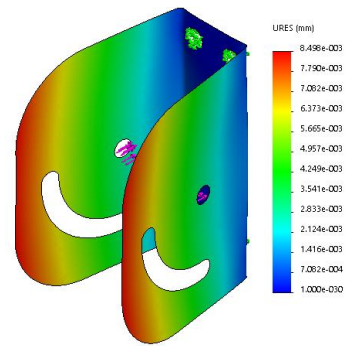


Fig. 11 Displacement distribution

4.2.2 Von Mises stress

Referring to the results provided by simulation in figure 12, we found that in areas of stress concentrations (having the red color).

There is a maximum of stress $\sigma_{\max} = 2.57 \text{ MPa}$.

$$\sigma_{\max} < \sigma_{\text{adm}} = \frac{R_c}{S} \approx 100 \text{ MPa} \quad (3)$$

where s is the safety coefficient.

We can approve that the clevises can bear the load of the solar collector.

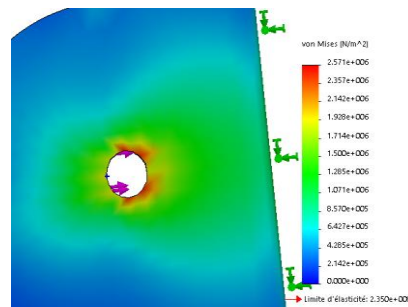
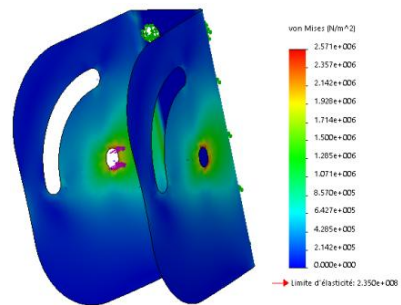


Fig. 12 Von Mises distribution

5. Conclusions

The design of a double pass solar air heaters fixed in the wall using a four legs pivoting system was presented. To verify the resistance of our support that assures the solar collector fixed on a wall and its resistance to weather conditions, a static analysis of the mounting brackets and the clevis was investigated using the CAD software Solid Works.

References

- [1] Daniels F., Duffie JA., Solar energy research. University of Wisconsin Press (1955).
- [2] Ong KS., Thermal performance of solar air heaters. mathematical model and solution procedures. *Sol Energy* (1995), 55:2 pp 93–109.
- [3] Bhushan B., Singh R., Thermal and thermo hydraulic performance of roughened solar air heater having protruded absorber plate. *Sol Energy* (2012), 86:3 pp 388–396.
- [4] Ammari H.D., A mathematical model of thermal performance of a solar air heater with slats. *Renew Energy* (2003), 28 pp 597–1615.
- [5] Shamardan M.M., Norouzi M., Kayhani M.H., Delouei A.A., An exact analytical. solution for convective heat transfer in rectangular ducts. *Appl Phys Eng Zhejiang Univ-Sci A* (2012), 13:10 pp 768–781.
- [6] Lee D.S., Hung T.C., Lin J.R., Zhao J., Experimental investigations on solar chimney for optimal heat collection to be utilized in organic Rankine cycle. *Appl. Energy* (2015), 154 pp 651–662.
- [7] Bassiouny R., Koura N.S.A., An analytical and numerical study of solar chimney use for room natural ventilation. *Energy Build.* (2008), 40 pp 865–873.
- [8] Dović D., Andrassy M., Numerically assisted analysis of flat and corrugated plate solar collectors thermal performances. *Sol. Energy* (2012), 86 pp 2416–2431.